Surface Chemistry

DOI: 10.1002/ange.201202318

Chemical Interface Damping in Single Gold Nanorods and Its Near Elimination by Tip-Specific Functionalization**

*Peter Zijlstra, Pedro M. R. Paulo, Kuai Yu, Qing-Hua Xu, and Michel Orrit**

A localized surface plasmon is the collective oscillation of the conduction electrons in a metal nanoparticle. The plasmon induces a strong absorption of light and significant emission, enabling the straightforward detection of individual particles in a far-field optical microscope.[1] A myriad of applications have arisen from the ability to detect a single particle, including optical antennas,[2,3] super-resolution localization and tracking of proteins conjugated to a metal particle,[4,5] and plasmonic biosensing with single-molecule sensitivity.[6,7]

Functionalization is often required to study specific interactions, a prime example is the detection of proteins by monitoring frequency shifts of the plasmon resonance.[6–8] Such functionalization is commonly achieved using thiol chemistry. The covalent thiol–gold bond securely attaches the receptor to the surface, but it also perturbs the conduction electron cloud in the particle. The reduced density of free electrons reduces the plasma frequency of the metal, resulting in a red-shift of the surface plasmon.[9] This red-shift is most pronounced in particles with a diameter < 20 nm because of their large fraction of surface atoms, and has been studied on colloidal suspensions.[10–12]

In these studies a line broadening was also observed because of an increased scattering rate of the conduction electrons by the modified potential on the particle surface. Such chemical interface damping provides an extra non-radiative decay channel for the plasmon resonance. The line broadening cannot be quantified using ensemble methods because of the inherent presence of size dispersion in these samples. More importantly, no strategies exist yet to control or eliminate chemical interface damping, which would be highly beneficial for applications such as plasmon sensing.

Here we employ single-particle spectroscopy to elucidate the effect of a thiol coating on the homogeneous linewidth of the longitudinal surface plasmon of gold nanorods. The line broadening we observe upon conjugation scales as the density of thiols on the surface of the particle. For the application as a plasmon sensor we developed a conjugation protocol to specifically functionalize the tips of a nanorod with biotin. This nearly eliminates chemical interface damping because of the reduced number of thiol groups on the side of the rod, while the sensitivity to the binding of streptavidin is maintained.

The gold nanorods employed in this study were synthesized using a wet-chemical method[13,14] that yielded nanoparticles with ensemble-average dimensions of 9 nm by 37 nm, and a longitudinal plasmon in water at approximately 760 nm (see the Supporting Information). To resolve individual nanorods in the optical microscope, we spin-coated the particles on a cleaned coverslip to a particle density of about 0.1 μm^{-2}. After spin-coating the substrate was UV/Ozone cleaned for 30 minutes to remove organic molecules such as surfactant from the particle surface. White-light spectra of individual particles were recorded in a flow cell using bright-field spectroscopy[1,15] (for details see the Supporting Information). As shown in Figure 1a, the presence of a particle in the light focus attenuates the beam because of the interference between the field scattered by the particle and the field reflected from the glass–water interface. We only analyzed particles that showed a single Lorentzian peak in the near-infrared, characteristic of a single gold nanorod in the focus.

In Figure 1a we show the background-corrected white-light spectrum of the same single nanorod immersed in phosphate-buffered saline (PBS) before and after coating with cysteamine, a thiol with a chain length of about 0.4 nm. The thiolation was achieved by incubating in a 1 mM solution of cysteamine in PBS for 1 hour, resulting in full coverage of the particle surface with thiols. The longitudinal plasmon of this particle red-shifted by 15 nm (30 meV) and broadened by 16 nm (32 meV). In Figure 1b and c we show the time dependence of the red-shift and the broadening, where we fitted the data with a single exponential decay with a characteristic time of about 5 minutes.

[*] P. Zijlstra, K. Yu, Prof. M. Orrit
MoNOS, Huygens Laboratorium, Universiteit Leiden
2300 RA Leiden (The Netherlands)
E-mail: orrit@physics.leidenuniv.nl

P. M. R. Paulo
Centro de Química Estrutural—Complexo I
Instituto Superior Técnico
Av. Rovisco Pais, 1049-001 Lisboa (Portugal)

K. Yu, Q.-H. Xu
Department of Chemistry and
NUS Graduate School for Integrative Sciences and
Engineering, National University of Singapore
Singapore, 117456 (Singapore)

P. Zijlstra
Current address:
Molecular Biosensors for Medical Diagnostics
Department of Applied Physics, Eindhoven University of Technology
Eindhoven, The Netherlands

[**] P.Z. and M.O. acknowledge financial support from the European Research Council (Advanced Grant SiMoSoMa). P.Z. acknowledges financial support from the Netherlands Organisation for Scientific Research (Veni Fellowship). P.M.R.P. acknowledges financial support from Program Ciência 2008 from the Fundação para a Ciência e a Tecnologia. K.Y. and Q.-H.X acknowledge support from the Faculty of Science, National University of Singapore (grant number R-143-000-341-112).

Supporting information for this article is available on the WWW under http://dx.doi.org/10.1002/anie.201202318.

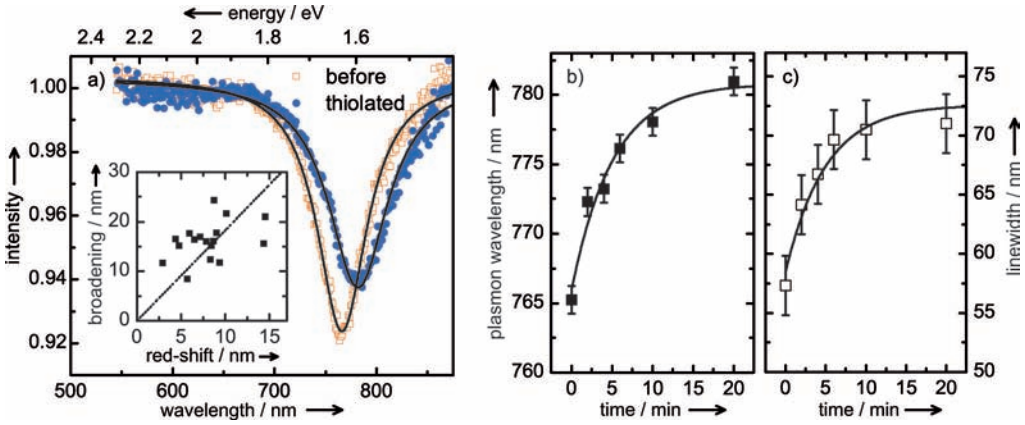

Figure 1. Broadening of the longitudinal plasmon caused by coating with the short-chain thiol cysteamine. a) White-light spectrum of a single particle before (orange squares) and after (blue circles) incubation in a 1 mM solution of cysteamine for 1 hour. The solid lines are lorentzian fits to the spectrum. The inset shows the correlation between the measured red-shift and broadening of the plasmon for several individual particles. The dotted line is a guide to the eye. b,c) Time-dependence of b) the wavelength and c) the linewidth of the longitudinal plasmon for the particle in (a). The solid lines are single-exponential fits with a characteristic time of about 5 min.

In the inset of Figure 1 a we show the correlation between the measured red-shift and broadening for several particles. For this short thiol we observe a weak correlation, whereas for longer thiol chains we did not observe any correlation. The absence of a strong correlation is expected because the red-shift depends on both the increased local refractive index due to the thiol backbone, and on the reduced density of free electrons in the particle due to the gold–thiol bond. The former effect strongly depends on the location of the molecule on the particle surface. Thiol groups at the tip generate a larger shift than those on the side faces because of the higher local field strength (see the inset in Figure 4 b). The line broadening on the other hand mainly depends on the number of thiol–gold bonds and is expected to be less sensitive to the location of the thiol on the particle surface.

From the accumulated statistics we find an average red-shift of 8 ± 3 nm (17 ± 7 meV) upon functionalization with cysteamine. Using the electrostatic model for a coated ellipsoid[16] immersed in water, we estimate that the increased refractive index because of the thiol backbone (thickness 0.4 nm, refractive index 1.45[17]) causes a red-shift of about 3 nm (about 6 meV, see the Supporting Information). The remaining red-shift of 5 nm (11 meV) is then caused by an effective reduction of the density of free electrons by about 1.5%. Because one gold atom provides one free electron, a 1.5% reduction is equivalent to about 1500 electrons for our particle volume of about 2×10^3 nm^3.

In our small particles the linewidth of the plasmon is determined by damping effects in bulk gold and by electron surface scattering.[18] The bulk damping term Γ_{bulk} equals about 77 meV, yielding a plasmon linewidth of about 35 nm at 750 nm.[19] Our data indicates that electron surface scattering increases the linewidth to 50 ± 5 nm (110 ± 10 meV), in good agreement with earlier reports.[18,20] After thiolation with cysteamine we find a linewidth of 65 ± 5 nm (143 ± 10 meV), indicating that chemical interface damping introduces an additional broadening of 15 nm (33 meV).

The effect of the chain length of the thiol backbone on the plasmon energy and linewidth is displayed in Figure 2. We do not observe a strong dependence of the red-shift on the chain length, likely because the shift is a function of the location of the thiol group on the surface of the particle, as well as the thickness and density of the layer. The line-broadening on the other hand is three-fold higher for the short-chain thiol group compared to the longest chain we investigated (thiolated polyethylene glycol, molecular weight = 5 kDa). This suggests that longer thiol molecules form a less dense monolayer because of steric hindrance and disorder caused by the chain.

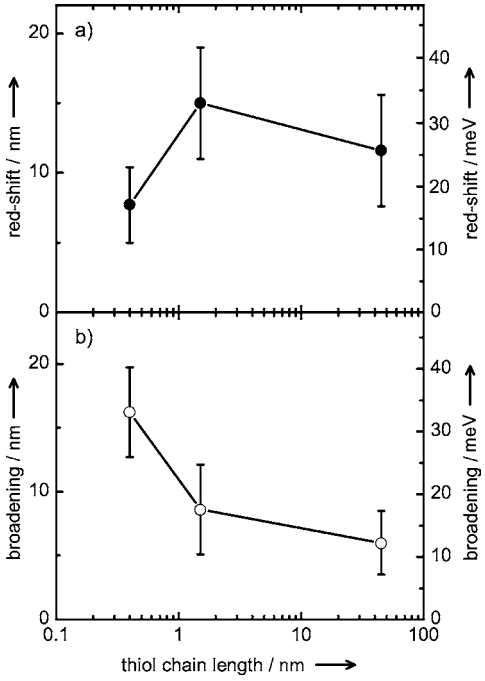

Figure 2. Plasmon red-shift and line broadening of single gold nanorods as functions of the chain length of the thiol molecule. The error bars indicate the standard deviation of the population.

The observed line-broadening adversely affects applications that rely on the high absorption and emission cross-section, the near-field enhancement, and the narrow linewidth of the plasmon. Here we focus on the application of plasmonic biosensing. The maximum sensitivity is obtained

when the analyte binds close to the particle surface because of the high local field strength. Typically the whole surface of a particle is functionalized with a short-chain thiol molecule,[8,21] causing significant chemical interface damping in small particles. We present a protocol (Figure 3) to specifically functionalize the tips of a nanorod only.[22–24] This minimizes the chemical interface damping by a reduced number of thiol–gold bonds, while it fully exploits the large field enhancement in the tip region.

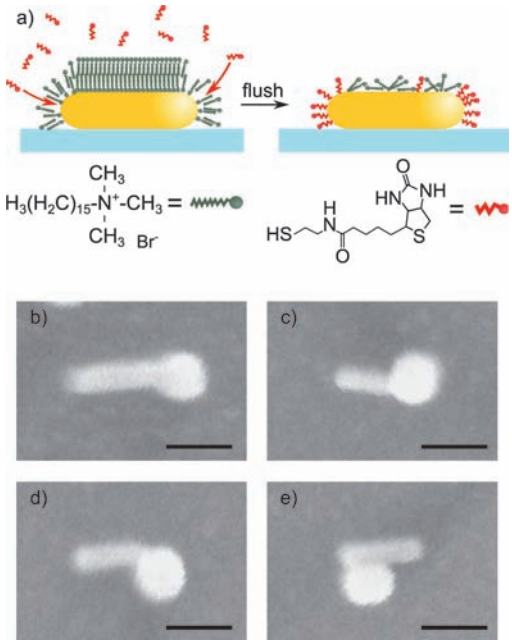

Figure 3. Tip-functionalization of nanorods immobilized on a substrate. a) Illustration of the functionalization protocol. b–e) Scanning electron microscopy images of gold nanorods that were tip-functionalized with biotin, and subsequently incubated in a 1 nM solution of streptavidin-coated gold nanospheres. 65% of the spheres were bound to the tip of a nanorod (b–d), whereas 35% bound to the side (e). The scale bars are 20 nm.

The immobilized nanorods were firstly incubated in a 2 mM solution of cetyltrimethylammonium bromide (CTAB) for 30 minutes. This establishes a bilayer of CTAB on the surface of the rod, which is less dense at the tips because of the small radius of curvature. The flow cell was then incubated in a 2 μM solution of thiolated biotin in PBS, in the presence of 2 mM CTAB. The dense CTAB bilayer on the side faces provides steric hindrance for the binding of thiolated biotin, resulting in a tip-specific functionalization.

To verify the functionalization of the tip, we incubated the flow cell with a 1 nM solution of streptavidin-functionalized gold spheres (Sigma, mean diameter 8–12 nm) for 1 hour. From electron microscopy analysis of 138 particles we find that 65% of the spheres bound to one of the tips of a nanorod, 35% being on the side (see Figure 3b–e). The majority of the particles that bound a sphere only exhibited a single sphere, likely because of the low concentration and comparatively slow diffusion of the streptavidin-coated spheres. Considering that the surface area of the sides of a spherically capped cylinder is 3.7 times larger than the tip area, we estimate that the density of biotin at the tip of the particle is approximately seven times larger than on the side faces (assuming that the probability to find a streptavidin-coated sphere is proportional to the surface density of biotin).

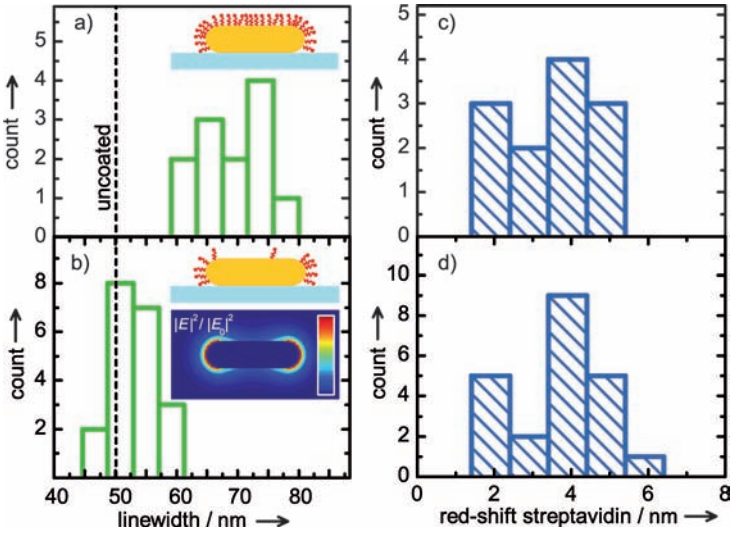

Figure 4. Homogeneous linewidth of the longitudinal plasmon of biotin-functionalized nanorods for a) full functionalization and b) tip-specific functionalization. The vertical dashed line indicates the average linewidth of the plasmon before the thiol-coating was applied. The functionalized nanorods were subsequently incubated in 100 nM streptavidin for 1 hour, and the peak-shifts of individual particles are indicated for c) full functionalization and d) tip-specific functionalization. The inset in (b) shows the local field intensity for a gold nanorod immersed in water, normalized to the intensity of the incoming field (calculated using the discrete dipole approximation). The color axis ranges from $|E|^2/|E_0|^2 = 1$–4000 on a linear scale.

We now compare the linewidth of fully functionalized gold nanorods with tip-specific functionalized particles. In Figure 4a we show the homogeneous linewidth of individual gold nanorods that are fully functionalized with biotin by first incutating in 1 mM cysteamine for one hour, followed by 1 mM of NHS-biotin (a biotinylation reagent; NHS = *N*-hydroxysuccinimide) for one hour. Chemical interface damping broadens the plasmon by about 18 nm to 67 ± 5 nm (150 ± 10 meV). As shown in Figure 4b the tip-specific functionalization does not induce a significant line broadening, and the linewidth is only about 3 nm (about 6 meV) broader than for the particles without functionalization.

We analyze the sensing performance of both functionalization strategies by determining the plasmon shift upon incubation in 100 nM streptavidin for 1 hour. The magnitude of the shift depends on the interaction strength between the plasmon and the proteins, given by 1) the refractive index contrast between the buffer ($n \approx 1.33$) and the proteins (typically $n = 1.45$ for a hydrated protein[25]) and 2) the local electric field intensity averaged over the volume of the proteins. The calculated electric field intensity for the longitudinal plasmon of a nanorod (inset of Figure 4b) is largest at the tips and reduces along the long edges of the particle. The total plasmon shift thus mainly depends on the number

of proteins that bind to the tips of the particle. As shown in Figure 4c,d the tip-functionalized particles show the same plasmon shift as the fully functionalized particles, indicating that for both cases the number of proteins that binds to the tips is similar.

We performed several blank measurements to verify the specifity of our tip-functionalized sensor (see the Supporting Information). For triethylene-glycol-functionalized particles we found a negligible plasmon shift of 0 ± 1 nm upon incubation in 100 nM streptavidin. We also investigated the plasmon shifts of biotin-functionalized particles in the presence of 100 nM of protein that lacks a binding pocket for biotin (i.e. streptavidin that was presaturated with biotin). Also in this case we did not observe a significant red-shift, establishing the specificity of the sensor.

Our results indicate that surface chemistry and optical properties of metal particles are intimately coupled. This highlights the importance of advanced functionalization protocols to obtain the desired functionality and optical response. We showed that the functionalization of specific sites nearly eliminates the effects of chemical interface damping, while maintaining the functionality of the particle coating. The extension of such strategies to other particle geometries will enable the full exploitation of the unique optical and chemical properties of single metal particles for applications in biophysics, photonics, and materials science.

Received: March 23, 2012
Revised: June 8, 2012
Published online: July 6, 2012

Keywords: nanoparticles · surface chemistry · surface plasmons

[1] P. Zijlstra, M. Orrit, *Rep. Prog. Phys.* **2011**, *74*, 106401.
[2] A. Kinkhabwala, Z. F. Yu, S. H. Fan, Y. Avlasevich, K. Müllen, W. E. Moerner, *Nat. Photonics* **2009**, *3*, 654 – 657.
[3] A. G. Curto, G. Volpe, T. H. Taminiau, M. P. Kreuzer, R. Quidant, N. F. van Hulst, *Science* **2010**, *329*, 930 – 933.
[4] R. Ishmukhametov, T. Hornung, D. Spetzler, W. D. Frasch, *EMBO J.* **2010**, *29*, 3911 – 3923.
[5] T. Fujiwara, K. Ritchie, H. Murakoshi, K. Jacobson, A. Kusumi, *J. Cell Biol.* **2002**, *157*, 1071 – 1081.
[6] P. Zijlstra, P. M. R. Paulo, M. Orrit, *Nat. Nanotechnol.* **2012**,*7*, 379 – 382.
[7] I. Ament, J. Prasad, A. Henkel, S. Schmachtel, C. Sönnichsen, *Nano Lett.* **2012**, *12*, 1092 – 1095.
[8] K. M. Mayer, J. H. Hafner, *Chem. Rev.* **2011**, *111*, 3828 – 3857.
[9] U. Kreibig, M. Vollmer, *Optical properties of metal clusters*, Springer, Berlin, **1995**.
[10] M. A. Garcia, J. de La Venta, P. Crespo, J. LLopis, S. Penadés, A. Fernández, A. Hernando, *Phys. Rev. B* **2005**, *72*, 241403.
[11] T. Linnert, P. Mulvaney, A. Henglein, *J. Phys. Chem.* **1993**, *97*, 679 – 682.
[12] S. Peng, J. M. McMahon, G. C. Schatz, S. K. Gray, Y. G. Sun, *Proc. Natl. Acad. Sci. USA* **2010**, *107*, 14530 – 14534.
[13] B. Nikoobakht, M. A. El-Sayed, *Chem. Mater.* **2003**, *15*, 1957 – 1962.
[14] P. Zijlstra, C. Bullen, J. W. M. Chon, M. Gu, *J. Phys. Chem. B* **2006**, *110*, 19315 – 19318.
[15] K. Lindfors, T. Kalkbrenner, P. Stoller, V. Sandoghdar, *Phys. Rev. Lett.* **2004**, *93*, 037401.
[16] C. F. Bohren, D. R. Huffman, *Absorption and scattering of light by small particles*, Wiley, New York, **1998**.
[17] F. S. Damos, R. C. S. Luz, L. T. Kubota, *Langmuir* **2005**, *21*, 602 – 609.
[18] C. Novo, D. Gomez, J. Pérez-Juste, Z. Y. Zhang, H. Petrova, M. Reismann, P. Mulvaney, G. V. Hartland, *Phys. Chem. Chem. Phys.* **2006**, *8*, 3540 – 3546.
[19] P. B. Johnson, R. W. Christy, *Phys. Rev. B* **1972**, *6*, 4370 – 7379.
[20] C. Sönnichsen, T. Franzl, T. Wilk, G. von Plessen, J. Feldmann, O. Wilson, P. Mulvaney, *Phys. Rev. Lett.* **2002**, *88*, 077402.
[21] G. J. Nusz, S. M. Marinakos, A. C. Curry, A. Dahlin, F. Höök, A. Wax, A. Chilkoti, *Anal. Chem.* **2008**, *80*, 984 – 989.
[22] K. K. Caswell, J. N. Wilson, U. H. F. Bunz, C. J. Murphy, *J. Am. Chem. Soc.* **2003**, *125*, 13914 – 13915.
[23] X. S. Kou, S. Z. Zhang, Z. Yang, C. K. Tsung, G. D. Stucky, L. D. Sun, J. F. Wang, C. H. Yan, *J. Am. Chem. Soc.* **2007**, *129*, 6402 – 6404.
[24] W. H. Ni, R. A. Mosquera, J. Pérez-Juste, L. M. Liz-Marzán, *J. Phys. Chem. Lett.* **2010**, *1*, 1181 – 1185.
[25] J. Vörös, *Biophys. J.* **2004**, *87*, 553 – 561.

